ENERGY CONSERVATION LAW IN THE PROBLEM OF ELASTIC PLATE IMPACT ONTO LIQUID FREE SURFACE

T.I.Khabakhpasheva, A.A.Korobkin

Lavrentyev Institute of Hydrodynamics,
Novosibirsk, 630090, RUSSIA

The plane unsteady problem of elastic plate impact onto shallow wave crest is considered. The liquid is assumed ideal and incompressible, and its motion plane and potential. The elastic plate is the bottom of a structure, which penetrates the liquid at a constant velocity V. The plate deflection is governed by the Euler beam equation and the beam edges are assumed simply supported. The problem is coupled because the liquid flow, the beam deflection and the geometry of the contact region between the entering body and the liquid must be determined at the same time. Details of the process, and the geometry of the contact region in particular, are essentially dependent on the initial free-surface shape, which is usually not well defined in practical problems. Even within simplified approaches, sophisticated numerical algorithms are required to describe the parameters of the contact region [1-6]. On the other hand, experiments [5] and the theory developed by Faltinsen [6] show that some important characteristics of the impact including the maximum of bending stresses in the plate are weakly dependent on the impact conditions. Moreover, the bending stresses approach their maximum values after the plate is totally wetted (penetration stage). This indicates that global characteristics of the process such as the energy of the plate-liquid system can be of help to obtain estimations of the maximum of bending stresses.

The aim of the present study is to derive reasonable estimations of the bending stress maximum with the help of the energy conservation law and to compare these estmations with the experimental data [5] and the results obtained by direct numerical simulation of the wave impact within the Wagner approach.

Formulation of the problem

Initially an elastic beam of length $2L$ touches the curved free surface of the liquid, shape of which is given by the equation $y = f(x)$, where $|(df/dx)(x)| \ll 1$, $-\infty < x < +\infty$. The liquid is at rest and occupies the region $y < f(x)$. The Cartesian coordinate system xOy is fixed in space and its origin coincides with the left-hand edge of the beam at the initial instant of time, $t = 0$. Then the beam starts to penetrate the liquid vertically with the velocities of its edges being V. The beam deflection $w(x,t)$, $0 < x < 2L$, is governed by the Euler beam equation and the liquid flow is described by the velocity potential $\varphi(x,y,t)$, which is connected with the hydrodynamic pressure $p(x,y,t)$ by the Cauchy-Lagrange integral. The velocity potential satisfies the Laplace equation in the flow domain $\Omega(t)$, which varies with time. External mass forces and surface tension are not taken into account. Both dimension and position of the contact region $D(t)$ are unknown in advance, which is the main feature of the impact problems. The boundary condition in the contact region $D(t)$ is taken in the form

$$\partial\varphi/\partial y = -V + w_t(x,t). \tag{1}$$

The kinematic and the dynamic ($p = 0$) conditions are hold on the liquid free surface.

Energy conservation law

Kinetic energy of the non-linear liquid flow $T_L(t)$ is given by

$$T_L(t) = -\int_0^t \left(\int_{D(\tau)} p \frac{\partial\varphi}{\partial y} ds \right) d\tau, \qquad T_L(t) = \int_{\Omega(t)} \int \frac{1}{2}\rho(\nabla\varphi)^2 dx dy, \tag{2}$$

where ρ is the liquid density. The Euler equation, which describes dynamics of the beam with simply supported edges, provides

$$T_B(t) + P_B(t) = \int_0^t \left(\int_{D(\tau)} p w_t ds \right) d\tau, \tag{3}$$

$$T_B(t) = \frac{1}{2} m_B \int_0^{2L} w_t^2(x,t) dx, \qquad P_B(t) = \frac{1}{2} EJ \int_0^{2L} w_{xx}^2(x,t) dx,$$

where $T_B(t)$ and $P_B(t)$ are the kinetic energy and the potential energy of the beam, respectively, m_B is the beam mass per unit length, E is the elasticity modulus and J is the inertia momentum of the beam cross-section.

Figure 1: Impact of an elastic beam on a curved liquid free surface. Initially, liquid is at rest, and the elastic plate just touches the free surface. The flow patterns after the impact are shown for different impact conditions (with and without a cavity formation).

Substituting (1) into equation (2) and combining (2) and (3), we obtain

$$T_B(t) + P_B(t) + T_L(t) = V \int_0^t F(\tau) d\tau, \tag{4}$$

where $F(t)$ is the total hydrodynamic force on the entering beam.

Wagner approach

The impact is the event of a short duration, which makes it possible to simplify the problem. Assuming that the maximum of bending stresses, which are of main interest in the present study, appears at a small penetration depth, when the deformations of the liquid region are still negligible compared to the beam length, we can, as a first approximation, put the boundary conditions on the line $y = 0$ and linearize them and the equations of motion near the initial rest state (Wagner approach). Nevertheless, even after all possible simplifications the problem is still complicated and difficult to treat. Main difficulties to describe the hydroelastic interaction are associated with the impact stage, during which the plate is wetted only partially. This is the stage, during which spray jets at the periphery of the contact region are observed. These jets are very thin and their contributions to both the flow in the main region and the contact region geometry are negligible but their kinetic energy is comparable with the energy of the main flow. At this stage the geometry of the contact region can be very complicated owing to both the plate deflection and the initial free-surface shape (figure 1). It is possible that a cavity on the plate surface is formed, which leads to high hydrodynamic loads at the moment of the cavity collapse. At the impact stage the problem is essentially nonlinear and its solution is very sensitive to the impact conditions. At the end of the impact stage, $t = t_*$, the beam is totally wetted and the spray jets continue to move inertially and separately from the main flow taking a part of the energy T_{jet} with them.

At the penetration stage the problem within the Wagner approach is linear and similar to the problem of floating plate vibration on the liquid free surface. The initial conditions for this problem come from the non-linear solution at the end of the impact stage. If the plate deflection and the velocities of its elements are known at $t = t_*$, then the characteristics of the process at the penetration stage, where the bending stresses take their maximum values, can be easily found. This observation indicates that the solution at the end of the impact stage is only required to evaluate the maximum of bending stresses in the plate.

During the penetration stage, $t > t_*$, the total kinetic energy of the liquid $T_L(t)$ can be presented as

$$T_L(t) = T_{jet} + T_{LR} + T_{LE}(t) - \rho V \int_0^{2L} \sqrt{x(2L-x)}\, w_t(x,t) dx, \tag{5}$$

where T_{LR} is the energy of the flow caused by the impact of the equivalent floating rigid plate at the velocity V (the boundary conditions for the corresponding velocity potential in the lower half-plane are: $\varphi_y = -V$, where $y = 0$, $0 < x < 2L$, and $\varphi = 0$, where $y = 0$, $x < 0$ and $x > 2L$), $T_{LE}(t)$ is the energy of the flow due to vibration of the floating elastic plate ($\varphi_y = w_t(x,t)$, where $y = 0$, $0 < x < 2L$, and $\varphi = 0$, where $y = 0$, $x < 0$ and $x > 2L$). The external work is given by

$$V \int_0^t F(\tau) d\tau = \frac{\pi}{2} \rho L^2 V^2 - \rho V \int_0^{2L} \sqrt{x(2L-x)}\, w_t(x,t) dx \tag{6}$$

within the Wagner approach. We obtain $T_{LR} = (\pi/4)\rho V^2 L^2$.

Substitution of (5) and (6) into (4) provides

$$T_B(t) + P_B(t) + T_{LE}(t) = \frac{\pi}{4} \rho V^2 L^2 - T_{jet} \qquad (t > t_*) \tag{7}$$

This means that the kinetic energy, which leaves the main flow region with the spray jets, is approximately equal to the energy of the flow caused by the floating plate impact and does not depend on initial shape of the free surface. Equation (7) also indicates that flexibility of entering body reduces the energy taken away with the spray jets.

Below we take the quantity $\frac{1}{2}\rho V^2 L^2$ as the energy scale and denote the terms on the left-hand side of the non-dimensionalized equations (7) by U_{kb}, U_{pb} and U_{kl}, respectively, and their sum by U_*. The energy equation (7) provides

$$U_* \leq \pi/2. \tag{8}$$

This inequality is used below instead of equation (7) to estimate the maximum of the bending stresses in the plate. This is because the jet energy T_{jet} is difficult to evaluate. In order to find this energy, we need to recover all details of the flow during the impact stage.

Numerical analysis

Direct numerical simulations of the impact stage were performed for different initial shapes of the free surface and different positions of the impact point (see figure 1) by the method of normal modes [1-4]. It was revealed that both the deflections and the velocities of the beam elements are essentially dependent on the initial free-surface shape during the impact stage. On the other hand, the 'elastic' energy $U_*(t_*)$ at the end of the impact stage is weakly dependent on the initial conditions.

At the penetration stage the total energy $U_*(t)$ remains constant, which follows from the fact that impact problem at the this stage is linear within the approximation employed. The parts of the 'elastic' energy $U_{kb}(t)$, $U_{pb}(t)$ and $U_{kl}(t)$ are functions of time and are depicted in figure 2 for the plate used in experiments [5] and the wave impact at the beam edge. The results of direct numerical simulations of the bending stresses in the plate, $\sigma(x,t) = -Ez_a w_{xx}(x,t)$, where z_a is the distance from the neutral axis in the beam cross-sectional area to the point where σ is evaluated (see [5]), are shown in figure 3, where the solid line is for the maximum of the non-dimensional stresses in the plate and the broken line is for the bending stresses at the plate centre. It is clear from this figure that the stresses at the plate centre can be used to estimate the absolute maximum value of stresses in the plate.

Figures 2 and 3 demonstrate that the main contribution to the 'elastic' energy at the beginning of the penetration stage comes from the kinetic energy of the liquid flow, $U_{kl}(t_*)$, but at the time instant t_{max}, when the bending stresses reach their maximum value, from the potential energy of the deformed plate, $U_{pb}(t_{max})$, with the kinetic energies $U_{kb}(t_{max})$ and $U_{kl}(t_{max})$ being negligibly small.

Within the normal mode approach the potential energy $U_{pb}(t)$, $t > t_*$, is the sum of contributions of each 'dry' mode. The relative contributions of the mode potential energies to the 'elastic' energy $U_*(t)$ are depicted in figure 4, where P_1 is the potential energy due to the first mode and P_2 is the contribution of the modes from second to tenth to the potential energy of the deformed plate. This figure shows that the one-mode approximation gives a reasonable estimation for the potential energy. On the other hand, this approximation underpredicts the maximum stresses as it is clear from figure 5, where the dotted curve is for the maximum stresses obtained within the one-mode approximation and the thick curve for stresses at the plate centre obtained with ten modes taken into account. Within the one-mode approximation the amplitude of the first mode and its first derivative in time are matched continuously with their values obtained numerically at the end of the impact stage, t_*, with ten modes taken into account.

The absolute maximum of the bending stresses σ_{max} and the time t_{max} can be found much easier if we observe that $P_1(t_{max}) \approx U_*$ at t_{max} (see figures 2 – 4). This approximate equality provides

$$\sigma_{max} \approx U_*^{\frac{1}{2}} V z_a \sqrt{\frac{E\rho L}{J}}, \qquad t_m \approx \frac{2L^2}{\pi}\sqrt{\frac{m_b + S_{11}\rho L}{EJ}}, \tag{9}$$

where $S_{11} = (\pi/2)[J_0^2(\pi/2) + J_1^2(\pi/2)]$ (see [1]). Equation (9) shows that t_{max} does not depend on the impact velocity, is proportional to $L^{5/2}$ and inverse proportional to $h^{3/2}$, where h is the plate thickness. The maximum of bending stresses σ_{max} is proportional to $(L/h)^{1/2}$ and the impact velocity V (see discussion of the experimental results in [5]). In the experiment conditions for the steel plate formulae (9) provide $\sigma_{max} = 1867\mu s$ and $t_{max} = 0.0075s$, which reasonably correspond to the measured values $\sigma_{max} = 1600\mu s$ and $t_{max} = 0,005s$. It should be noted that the connection between the elastic plate and the structure was more complicated in the experiment that it is employed in the simplified theoretical analysis here. Taking into account more realistic edge conditions reduces the differencies between the estimated and the measured values.

The non-dimensional 'elastic' energy U_* in (9) has to be evaluated from the numerical solution of the original problem at the impact stage with all peculiarities of this stage taken into account. This fact reduces the practical

(8) to estimate the stresses. The corresponding bound is depicted in figure 3 by the broken line.

Let us denote the total length of the beam by L_B, then (8) and (9) lead to

$$\frac{|\sigma_{max}|}{\left(\frac{z_a}{L_B}\right)V}\sqrt{\frac{J}{\rho E L_B^3}} \le \sqrt{\frac{\pi}{4}},$$

where $\sqrt{\pi/4} \approx 0.88$. Experimental results for the same ratio and different impact velocities, plates and impact conditions [5] provide its upperbound as 0.7 . The theoretical estimation obtained overpredicts the experimental estimation but is simple and can be recommended for structural analysis of plates subject to wave impact loads.

This research was supported by Russian Foundation for Basic Research Grant N 96-01-01767 and by SD RAS integrate project N 43.

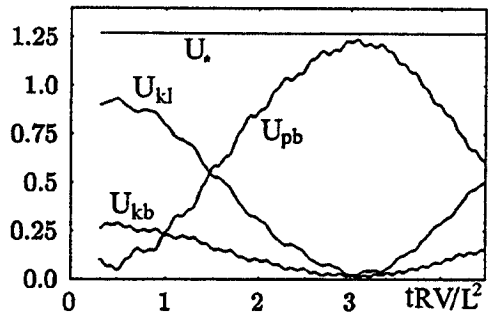

Figure 2: Components of the 'elastic' energy $U_*(t)$ as functions of time during the penetration stage

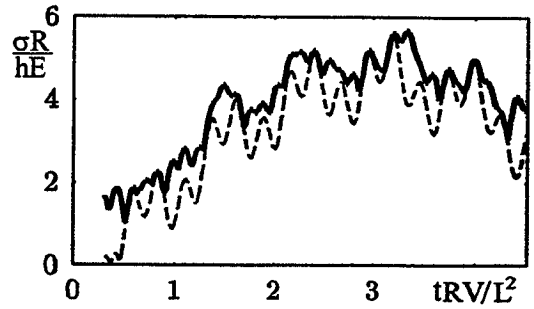

Figure 3: Non-dimensional stresses in the plate during the penetration stage: solid line is for maximum stress, broken line is for the bending stresses at the plate centre.

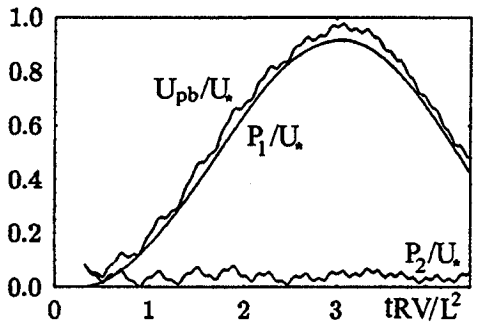

Figure 4. Relative contributions to the 'elastic' energy $U_*(t)$ of the total potential energy, U_{pb}/U_*; the potential energy due to the first mode, P_1/U_*; the potential energy due to the modes from second to tenth, P_2/U_*.

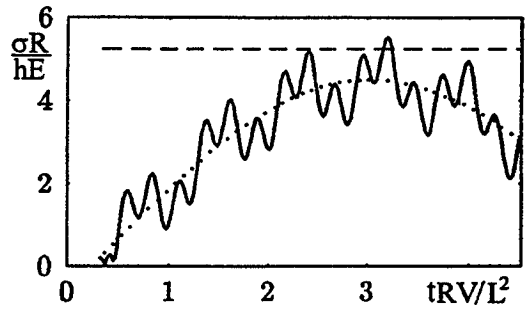

Figure 5. Non-dimensional stresses in the plate during the penetration stage: solid line is for bending stresses at the centre, broken line is the theoretical estimation of the bending stresses, dotted line is for bending stresses given by one-mode approximation.

References

1. Korobkin A. A. Wave impact on the centre of an Euler beam. J.Appl.Mech.Tech.Phys. 1998. V.39. N 5. P. 134-147.

2. Korobkin A.A., Khabakhpasheva T.I. Plane problem on unsymmetrical wave impact onto elastic plate. J.Appl.Mech.Tech.Phys. 1998. V.39. N 5. P. 148-158.

3. Khabakhpasheva T.I., Korobkin A.A. Wave impact on elastic plates. Proc. 12th Intern. Workshop on Water Waves and Floating Bodies, Carry-le-Rouet, France, 1997. P. 135-138.

4. Khabakhpasheva T.I., Korobkin A.A. One-side inequalities in the problem of the wave impact. Proc. 13th Intern. Workshop on Water Waves and Floating Bodies. Alphen aan den Rijn, Netherlands. 1998. P.67-70.

5. Faltinsen O. M., Kvålsvold J., Aarsnes J.V. Wave impact on a horizontal elastic plate. J.Marine Science and Technology. 1997. V. 2. N. 2. P.87-100.

6. Faltinsen O.M. The effect of hydroelasticity on ship slamming. Phil. Trans. R. Soc. London. 1997. A355. P.575-593.